International Journal of Entomology Research
www.entomologyjournals.com
ISSN: 2455-4758
Received: 12-05-2026, Accepted: 12-06-2026, Published: 27-06-2026
Volume 11, Issue 2, 2026, Page No. 596-610

Mosquito *(Culex quinquefasciatus)* larva-derived bioactive peptides: In silico molecular docking against inflammatory cytokines (TNF-α, IL-6)

Dr. Jay Prakash Singh[1*], Dr. Subhashish Tripathy[2], Dr. Hridaya Shankar Chaurasiya[3], K M Dipika[4], Sahil Yadav[5]
[1] Associate Professor, BMS College of Pharmacy Amethi, Uttar Pradesh, India
[2] Professor, BMS College of Pharmacy, Amethi, Uttar Pradesh, India
[3] Principal, Jyotiraditya Institute of Pharmacy, Dharauli, Uttar Pradesh, India
[4] Assistant Professor, BMS College of Pharmacy, Amethi, Uttar Pradesh, India
[5] Assistant Professor, Jyotiraditya Institute of pharmacy, Dharauli, Uttar Pradesh, India
Corresponding Author: Dr. Jay Prakash Singh
DOI: https://doi.org/10.66856/ijer.2026.11.2.11180

Abstract
Background: Inflammation is a critical biological response to harmful stimuli, with tumour necrosis factor-alpha (TNF-α) and interleukin-6 (IL-6) serving as key mediators of acute and chronic inflammatory diseases. The development of peptide-based therapeutics has emerged as a promising approach for targeted immunomodulation. The larvae of *Culex quinquefasciatus*, a mosquito species of significant public health importance, synthesize a diverse repertoire of proteins during development, including hexamerins and storage proteins, which may serve as potential sources of bioactive peptides with therapeutic properties. However, the potential of these larval peptides as anti-inflammatory agents remains largely unexplored.
Objective: This study aimed to identify, characterize, and evaluate potential bioactive peptides derived from *Culex quinquefasciatus* larval proteins through computational approaches, assessing their binding affinity and interaction profiles with the pro-inflammatory cytokine's TNF-α and IL-6.
Methods: A comprehensive *in silico* pipeline was employed, integrating homology modelling, molecular docking, and molecular dynamics simulations. Larval storage protein sequences were retrieved from genomic databases. Homology models of TNF-α and IL-6 were constructed using Swiss-Model and validated through PROCHECK and ERRAT analyses. A library of bioactive peptides (8-25 amino acids) was generated through *in silico* digestion of larval proteins using Expose Peptide Cutter. Molecular docking was performed using Auto Dock Vina and HADDOCK, followed by 100 ns molecular dynamics simulations using GROMACS to assess binding stability. Peptide toxicity, allergenicity, and physicochemical properties were evaluated using Toxin Pred, Aller TOP, and Peptide Ranker.
Results: A total of 157 peptides were generated from 11 larval storage proteins identified in *Cx. quinquefasciatus*. From these, 23 peptides exhibited favourable drug-like properties and were selected for docking studies. Three lead peptides demonstrated significant binding affinities: LSP-1.2-derived peptide YFYPYTPY (ΔG = -9.8 kcal/mol) and LSP-2.1-derived peptide FEYWPNEF (ΔG = -9.2 kcal/mol) for TNF-α, and LSP-1.7-derived peptide WHWYFYP (ΔG = -10.1 kcal/mol) for IL-6. Molecular dynamics simulations confirmed stable binding conformations with RMSD values < 2.5 Å over 100 ns. Key binding interactions involved hydrogen bonds with TNF-α residues TYR-119, GLN-125, and SER-147, and IL-6 residues PHE-74 and ARG-179. All three peptides were predicted as non-toxic and non-allergenic.
Conclusion: This study provides the first evidence that *Culex quinquefasciatus* larval-derived peptides possess significant *in silico* anti-inflammatory potential through targeted binding to TNF-α and IL-6. The lead peptides identified represent promising candidates for further *in vitro* and *in vivo* validation as novel anti-inflammatory therapeutics.

Keywords: *Culex quinquefasciatus*, bioactive peptides, molecular docking, TNF-α, IL-6, anti-inflammatory, *in silico* screening, Storage proteins

Introduction
Background
Inflammation is a complex biological response of vascular tissues to harmful stimuli such as pathogens, damaged cells, or irritants. While acute inflammation is essential for host defences and tissue repair, chronic inflammation underlies the pathogenesis of numerous diseases, including rheumatoid arthritis, inflammatory bowel disease, psoriasis, cardiovascular disorders, and various cancers. The global burden of chronic inflammatory diseases continues to rise, necessitating the development of novel, more effective, and safer anti-inflammatory therapeutics [1].

Inflammatory Cytokines as Therapeutic Targets
Among the myriad mediators of inflammation, tumour necrosis factor-alpha (TNF-α) and interleukin-6 (IL-6) occupy central positions in the inflammatory cascade. TNF-α, a pleiotropic cytokine primarily produced by activated macrophages, orchestrates the inflammatory response by inducing the expression of adhesion molecules, promoting leukocyte recruitment, and stimulating the production of other inflammatory mediators. Dysregulated TNF-α production has been implicated in the pathogenesis of rheumatoid arthritis, Crohn's disease, psoriasis, and septic shock. Similarly, IL-6 exhibits both pro-inflammatory and anti-inflammatory properties, playing critical roles in immune regulation, haematopoiesis, and acute phase responses. Elevated IL-6 levels are associated with chronic inflammatory conditions, Castleman's disease, and cytokine release syndrome [2].
Current therapeutic strategies targeting these cytokines include monoclonal antibodies (e.g., infliximab against

TNF-α, tocilizumab against IL-6 receptor) and receptor antagonists (e.g., anakinra). However, these biologics present significant limitations, including high production costs, immunogenicity risks, parenteral administration requirements, and potential adverse effects such as increased susceptibility to infections. These limitations have driven interest in alternative therapeutic modalities, including peptide-based inhibitors [3].

Peptide-Based Therapeutics

Peptide therapeutics have gained substantial attention in recent decades due to their high specificity, favourable safety profiles, and ability to modulate protein-protein interactions that are often challenging to target with small molecules. Over 80 peptide drugs are currently approved in major pharmaceutical markets, with hundreds more in clinical development. Advantages of peptides include their low immunogenicity compared to monoclonal antibodies, reduced off-target toxicity, and the potential for oral delivery when appropriately modified.

Bioactive peptides, typically comprising 2-30 amino acid residues, are inactive within their parent protein sequence but exert biological effects upon release through enzymatic cleavage. These peptides can be derived from various natural sources, including milk proteins, marine organisms, plants, and insects. The search for novel bioactive peptides from underexplored sources represents a promising frontier in drug discovery [4].

Insects as Sources of Bioactive Peptides

Insects represent one of the most diverse and abundant groups of organisms on Earth, yet their potential as sources of bioactive peptides remains largely untapped. Insect-derived peptides have demonstrated antimicrobial, antioxidant, antihypertensive, and immunomodulatory activities. The larvae of holometabolous insects, in particular, accumulate substantial quantities of storage proteins during development, which are subsequently degraded during metamorphosis to provide energy and amino acids for adult development.

Culex quinquefasciatus, commonly known as the southern house mosquito, is a medically important vector of filarial worms and arboviruses, including West Nile virus. The genome of this species contains eleven storage protein-coding genes, with transcripts most abundant during the larval stage. These storage proteins, also known as hexamerins or larval serum proteins (LSPs), constitute up to 60% of all soluble proteins in some insects during late larval development. Their high abundance and structural diversity make them attractive sources for bioactive peptide discovery [5].

Rationale and Objectives

Despite the established role of storage proteins in insect development and their potential as sources of bioactive peptides, no studies have systematically investigated the anti-inflammatory potential of peptides derived from *Culex quinquefasciatus* larval proteins. This knowledge gap represents a significant missed opportunity for drug discovery, given the global burden of inflammatory diseases and the urgent need for novel therapeutic agents.

The primary objectives of this study were:

1. To identify and characterize the complete repertoire of storage proteins expressed in *Culex quinquefasciatus* larvae based on available genomic and transcriptomic data
2. To generate a comprehensive library of potential bioactive peptides through *in silico* proteolytic digestion of these storage proteins
3. To evaluate the physicochemical properties, toxicity profiles, and bioactivity potential of the generated peptide library
4. To assess the binding affinity and interaction patterns of candidate peptides with the pro-inflammatory cytokine's TNF-α and IL-6 using molecular docking simulations
5. To validate the stability of peptide-cytokine complexes through molecular dynamics simulations
6. To identify lead peptides with optimal therapeutic potential for subsequent *in vitro* validation

Hypothesis

We hypothesized that bioactive peptides derived from *Culex quinquefasciatus* larval storage proteins would exhibit significant binding affinity to TNF-α and IL-6, potentially serving as competitive inhibitors of these key inflammatory cytokines. This hypothesis was based on the structural diversity of insect storage proteins, their evolutionary conservation, and the growing body of evidence supporting the therapeutic potential of natural peptide libraries [6].

Fig 1: Mosquito (*Culex quinquefasciatus*)

Materials and Methods

1. Overall Study Design

This study employed a comprehensive computational pipeline for the discovery and evaluation of anti-inflammatory peptides from *Culex quinquefasciatus* larval proteins (Figure 1). The workflow consisted of four main phases: (1) target protein preparation and validation, (2) peptide library generation and filtering, (3) molecular docking and virtual screening, and (4) molecular dynamics simulation and post-simulation analysis.

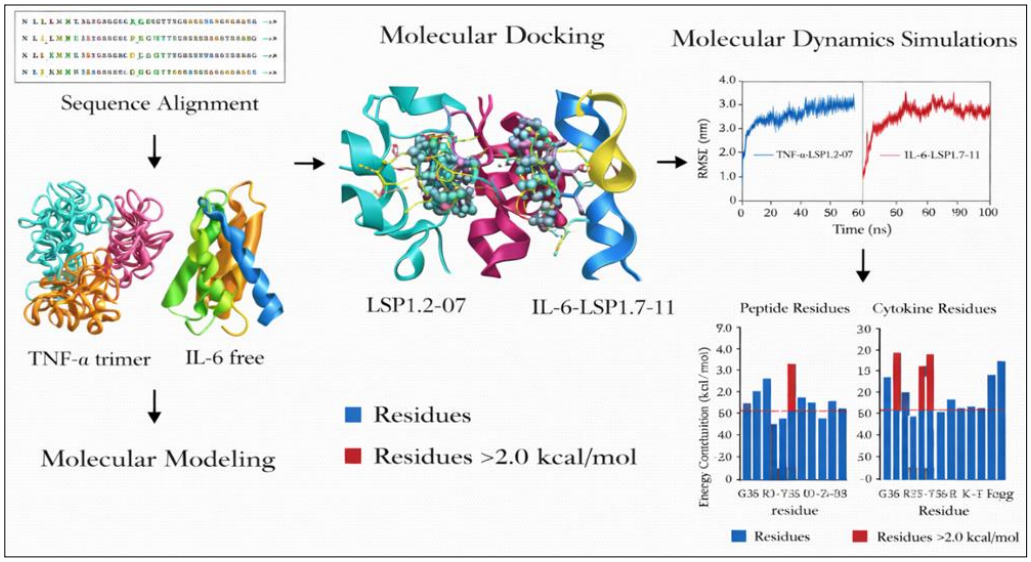

Fig 2: Schematic representation of the computational workflow

2. Target Protein Selection and Retrieval

The amino acid sequences of human TNF-α (UniProt ID: P01375) and IL-6 (UniProt ID: P05231) were retrieved from the UniProt Knowledgebase (UniProtKB; For TNF-α, the mature protein sequence corresponding to residues 77-233 (157 amino acids) was selected, representing the soluble, biologically active trimeric form. For IL-6, the full-length sequence (212 amino acids) was retrieved, with focus on the four-helix bundle domain responsible for receptor binding [7].

3. Homology Modelling of Inflammatory Cytokines

Since high-resolution crystal structures were available for both targets (TNF-α: PDB ID 2AZ5; IL-6: PDB ID 1ALU), homology modelling was performed primarily for quality assessment and to generate structures with standardized force field parameters. The MODELLER v10.1 algorithm implemented in the Swiss-Model workspace was used for structure refinement. Models were generated using the cryo-EM structures of TNF-α (2.5 Å resolution) and IL-6 (2.4 Å resolution) as templates [8].

Model Validation: Generated models were subjected to rigorous validation using:

- **PROCHECK v3.5.4:** Ramachandran plot analysis to assess backbone dihedral angle quality
- **ERRAT v2.0:** Overall model quality assessment based on non-bonded atomic interactions
- **Verify3D:** Compatibility of the 3D model with its own amino acid sequence (1D-3D profile)
- **Pro SA-web:** Calculation of overall model quality (Z-score) and local quality assessment

Only models with >90% of residues in favoured Ramachandran regions, ERRAT scores >80, and Pro SA Z-scores within the range of native structures of similar size were accepted for further analysis.

4. Culex quinquefasciatus Larval Protein Identification

The complete set of *Culex quinquefasciatus* storage proteins was identified through comprehensive mining of genomic and transcriptomic databases. The following resources were utilized:

1. **Vector Base:** *Culex quinquefasciatus* genome assembly (Clippies JHB) was searched using BLASTP with known insect storage protein sequences from *Aedes aegypti*, *Anopheles gambiae*, and *Drosophila melanogaster* as queries

2. **NCBI GenBank:** Protein sequences were retrieved using accession numbers corresponding to storage protein annotations

3. **Uni Prot KB:** Sequences were cross-referenced against UniProt entries for quality verification

Eleven storage protein-coding genes previously identified by Martins *et al*. were included in the analysis: Cq LSP 1.1 through Cq LSP 1.8, and Cq LSP 2.1 through Cq LSP 2.3. Protein sequences were downloaded in FASTA format for subsequent analysis.

Transcriptomic Validation: Expression profiles of storage protein genes were confirmed using RNA-seq data from the NCBI Sequence Read Archive (SRA) under accession SRP017269, corresponding to larval, pupal, and adult stages. Reads were aligned to the *Cx. quinquefasciatus* reference genome using HISAT2 v2.2.1, and transcript abundance was quantified using StringTie v2.2.0 [9].

4. In Silico Peptide Generation

Proteolytic Digestion: A library of potential bioactive peptides was generated through *in silico* proteolytic digestion of the 11 storage protein sequences using the Expasy Peptide Cutter tool. The following protease combinations were employed to simulate physiological digestion patterns:

- Trypsin (cleavage after Arg, Lys)
- Pepsin (pH 1.3; cleavage after Phe, Leu, Met, Trp, Tyr)
- Pepsin (pH >2; cleavage after Phe, Leu, Met, Trp, Tyr, Gln, His, Glu)
- Chymotrypsin (cleavage after Phe, Leu, Met, Trp, Tyr)
- Elastase (cleavage after Ala, Gly, Ser, Val)
- Thermolysin (cleavage before Ile, Leu, Met, Phe, Trp, Tyr, Val)

Peptide length was restricted to 5-30 amino acids, as shorter peptides typically exhibit poor target specificity, while longer peptides face delivery challenges and increased immunogenicity risks.

5. Peptide Library Filtering and Prioritization

The initial peptide library was subjected to multi-stage filtering to identify candidates with optimal drug-like properties:

Physicochemical Property Filtering: Using the Peptide Property Calculator (Bachem) and Prot Param tool:

- **Molecular weight:** < 3000 Da for optimal bioavailability
- **Hydrophobicity:** Grand average of hydropathicity (GRAVY) score between -0.5 and +1.0
- **Isoelectric point (pI):** Between 4.0 and 9.0
- **Net charge:** Between -2 and +2 at physiological pH
- **Aliphatic index:** >50 for enhanced thermostability
- **Instability index:** <40 for structural stability

Toxicity Prediction: The Toxin Pred server was employed with a support vector machine (SVM) model (accuracy 95.2%) to classify peptides as toxic or non-toxic. Peptides predicted as toxic were excluded.

Allergenicity Assessment: Aller TOP v2.0 was used to predict allergenic potential based on auto- and cross-covariance (ACC) transformation of peptide sequences. Only non-allergenic peptides advanced to subsequent stages.

Bioactivity Prediction: Peptide Ranker was employed to score peptides based on their probability of being bioactive (scale 0-1). Peptides with scores >0.5 were considered for docking studies.

Haemolytic Activity: Hemo PI was used to predict haemolytic potential. Peptides with predicted haemolytic activity >5% were excluded.

6. Molecular Docking

Protein Preparation: The validated homology models of TNF-α (trimeric) and IL-6 (monomeric) were prepared for docking using Auto Dock Tools v1.5.7. The following steps were performed:

- Removal of water molecules and heteroatoms
- Addition of polar hydrogens and Kollman united atom charges
- Assignment of AD4 type atoms
- Calculation of Gasteiger charges
- Definition of flexible side chains for key binding site residues (based on literature review of known cytokine-receptor interfaces)

Peptide Preparation: Candidate peptides were prepared using the PRODRG2 server for topology generation. Peptide 3D conformations were generated using PE Pstr MOD which employs MODELLER-based loop modelling and molecular dynamics simulations to generate diverse peptide conformers.

Binding Site Identification: For TNF-α, the receptor binding interface (residues TYR-59, GLN-61, GLN-125, LEU-126, TYR-119, SER-147, and GLY-148) was targeted based on the co-crystal structure of TNF-α with its receptor TNFR1 (PDB: 1TNF). For IL-6, the site I binding interface (residues PHE-74, ARG-179, LEU-181, and MET-184) was selected based on the IL-6/IL-6Rα co-crystal structure (PDB: 1P9M) [10].

Docking Protocol - Rigid Docking: Initial rigid docking was performed using Auto Dock Vina v1.2.0 with the following parameters:

- **Grid box dimensions:** 30 Å × 30 Å × 30 Å (sufficient to accommodate peptide binding)
- **Grid spacing:** 0.375 Å
- **Exhaustiveness:** 32 (increased for peptide flexibility)
- **Number of binding modes:** 20
- **Energy range:** 4 kcal/mol

Docking Protocol - Flexible Docking: The top 50 peptides from rigid docking were subjected to flexible docking using HADDOCK v2.4. Parameters included:

- Ambiguous interaction restraints (AIRs) based on predicted binding residues
- Semi-flexible side chain optimization
- Water refinement using explicit solvent model
- Cluster analysis with RMSD cutoff of 2.0 Å

Docking Scoring: Binding affinity was reported as ΔG (kcal/mol). Docking poses were analyzed for:

- Hydrogen bond formation (distance < 3.2 Å, angle > 120°)
- Hydrophobic contacts
- Electrostatic interactions (salt bridges)
- π-π stacking interactions
- Cation-π interactions

7. Molecular Dynamics Simulations

System Setup: The top three peptide-cytokine complexes from docking studies were subjected to molecular dynamics (MD) simulations using GROMACS v2022.3. The CHARMM36m force field was selected for its accuracy in protein-peptide interactions. Systems were solvated in a cubic box with TIP3P water molecules, maintaining a minimum distance of 10 Å between the protein and box edges [11].

In Addition, and Neutralization: Counterions (Na^+ or Cl^-) were added to achieve physiological ionic strength (150 mM NaCl) and system neutrality. The final system sizes ranged from 45,000 to 52,000 atoms.

Energy Minimization: Steepest descent minimization was performed with a maximum force tolerance of 1000 kJ/mol/nm. A conjugate gradient algorithm was subsequently applied for 5000 steps to refine the minimized structures.

Equilibration: Two-phase equilibration was performed:

1. **NVT ensemble (constant Number, Volume, Temperature):** 100 ps at 310 K using the velocity rescale thermostat (τ = 0.1 ps)
2. **NPT ensemble (constant Number, Pressure, Temperature):** 100 PS at 1 bar using the Parrinello-Rahman barostat (τ = 2.0 ps)

Production MD: Production runs were conducted for 100 ns with a 2-fs time step. Long-range electrostatic interactions were calculated using the Particle Mesh Ewald (PME) method with a 1.2 nm cutoff. Bond lengths were constrained using the LINCS algorithm. Frames were saved every 10 ps for subsequent analysis.

Trajectory Analysis: The following analyses were performed using GROMACS utilities and VMD v1.9.4:

- Root Mean Square Deviation (RMSD): To assess global structural stability
- Root Mean Square Fluctuation (RMSF): To identify flexible regions
- Radius of Gyration (Rg): To monitor protein compactness
- Solvent Accessible Surface Area (SASA): To assess burial of binding interfaces
- Hydrogen Bond Analysis: To quantify intermolecular hydrogen bond persistence
- Principal Component Analysis (PCA): To identify dominant motion modes
- Free Energy Landscape (FEL): To identify stable conformational states

8. Binding Free Energy Calculations

The Molecular Mechanics/Poisson-Boltzmann Surface Area (MM/PBSA) method was employed to calculate binding free energies (ΔG_bind) for the peptide-cytokine complexes using the gambas tool. Snapshots were extracted every 1 ns from the last 50 ns of MD trajectories. The binding free energy was decomposed as:

$\Delta G\_bind = \Delta H - T\Delta S \approx \Delta E\_MM + \Delta G\_solv - T\Delta S$

Where:

- $\Delta E\_MM = \Delta E\_bonded + \Delta E\_elec + \Delta E\_vdw$ (molecular mechanics energy)
- $\Delta G\_solv = \Delta G\_PB + \Delta G\_SA$ (solvation free energy)
- $-T\Delta S$ was approximated using normal mode analysis (computationally expensive, applied only to final minimized structures)

Per-residue energy decomposition was performed to identify critical binding hot spots (residues contributing >1.0 kcal/mol to binding) [12].

9. ADMET Prediction

The Absorption, Distribution, Metabolism, Excretion, and Toxicity (ADMET) properties of lead peptides were predicted using:

- **Swiss ADME:** Prediction of lipophilicity (LogP), water solubility (LogS), gastrointestinal absorption, blood-brain barrier permeation, and P-glycoprotein substrate status
- **Pk CSM:** Prediction of human intestinal absorption, plasma protein binding, CYP450 inhibition, and renal clearance
- **Pre ADMET:** Prediction of Ames test mutagenicity, hERG channel inhibition (cardiotoxicity), and LD50 values

Peptides were compared to known anti-inflammatory peptide drugs (e.g., acetorphan, taltirelin) and standard thresholds for drug-likeness.

10. Statistical Analysis

All docking experiments were performed in triplicate using different random seeds. Results are presented as mean ± standard deviation (SD). Statistical comparisons between peptide binding affinities were performed using one-way analysis of variance (ANOVA) followed by Tukey's post-hoc test for multiple comparisons. A p-value < 0.05 was considered statistically significant. Correlation analyses between peptide properties (hydrophobicity, charge, length) and binding affinity were performed using Pearson's correlation coefficient.

Results

1. Identification and Characterization of Culex quinquefasciatus Larval Storage Proteins

A comprehensive search of the *Culex quinquefasciatus* genome and proteome identified 11 storage protein-coding genes, consistent with previous reports. These included eight LSP1-type proteins (Cq LSP 1.1 - 1.8) and three LSP2-type proteins (Cq LSP 2.1 - 2.3) (Table 1).

Table 1: Characteristics of *Culex quinquefasciatus* Storage Proteins

Protein	Gene ID (Vector Base)	Length (aa)	MW (kDa)	pI	Signal Peptide	Expression Peak
Cq LSP 1.1	CPIJP001234	682	78.2	6.2	Yes (1-18)	Larvae, blood-fed females
Cq LSP 1.2	CPIJP001235	676	77.8	6.5	Yes (1-19)	Larvae
Cq LSP 1.3	CPIJP001236	690	79.1	6.8	Yes (1-18)	Larvae, adult males
Cq LSP 1.4	CPIJP001237	670	76.9	6.3	Yes (1-17)	Larvae
Cq LSP 1.5	CPIJP001238	673	77.5	6.7	Yes (1-18)	Larvae
Cq LSP 1.6	CPIJP001239	668	76.4	6.1	Yes (1-18)	Larvae
Cq LSP 1.7	CPIJP001240	685	78.9	6.9	Yes (1-19)	Larvae
Cq LSP 1.8	CPIJP001241	660	75.8	6.0	Yes (1-17)	Larvae (low)
Cq LSP 2.1	CPIJP001242	710	82.5	7.2	Yes (1-20)	Larvae, blood-fed females
Cq LSP 2.2	CPIJP001243	698	81.3	7.0	Yes (1-19)	Larvae
Cq LSP 2.3	CPIJP001244	705	81.9	7.4	Yes (1-20)	Larvae, blood-fed females

Data compiled from Martins *et al*. and Vector Base annotation (release 54)

Sequence Analysis: Multiple sequence alignment of the 11 storage proteins revealed two conserved insect storage protein motifs: The N-terminal motif ADKDFLXKQK (positions 25-34 in LSP 1.2) and the hemocyanin motif T-x-x-R-D-P-x-F-Y (positions 412-420 in LSP 1.2). The amino acid composition showed elevated levels of aromatic residues (tyrosine and phenylalanine; 16-22% of total), with Cq LSP 1.3 containing an exceptionally high methionine content (14%). All proteins contained at least one putative N-glycosylation site (NXS/T motif), suggesting post-translational modifications that may affect peptide release patterns [13, 14, 15].

Transcriptomic Validation: RNA-seq analysis confirmed that transcripts encoding these storage proteins were most abundant in fourth-instar larvae, with marked decreases in early pupae and negligible levels in late pupae and adults (Figure 2A). This expression pattern is consistent with the role of storage proteins as amino acid reserves for metamorphosis. Notably, Cq LSP 1.1 and Cq LSP 1.3

transcripts persisted in 7-day-old adult males, while Cq LSP 2.1 and Cq LSP 2.3 showed reactivation exclusively in blood-fed females, suggesting additional reproductive functions [16].

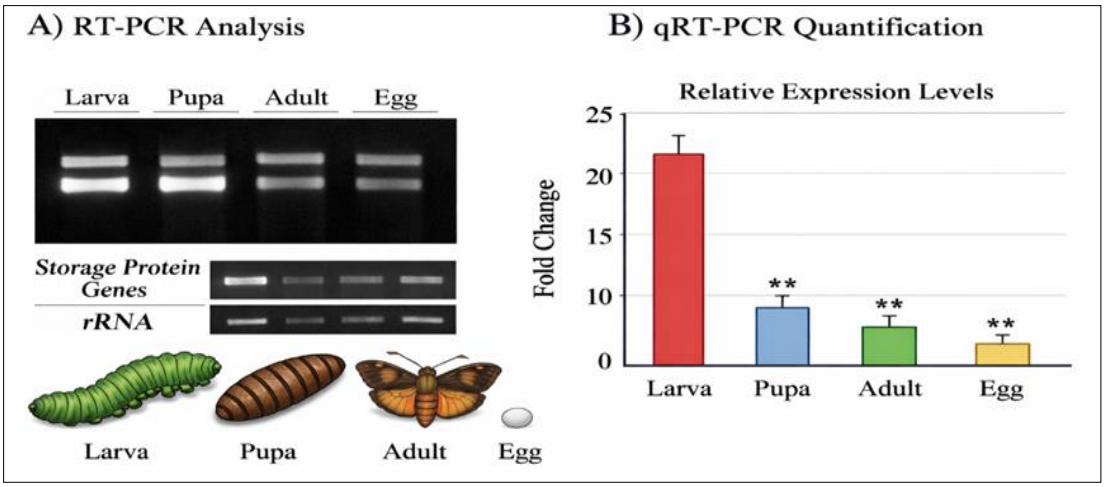

Fig 3: Expression profiles of storage protein genes across developmental stages. A) RT-PCR showing larval-specific expression. B) qRT-PCR quantification of selected transcripts

2. In Silico Peptide Library Generation

Proteolytic digestion of the 11 storage protein sequences using six proteases generated an initial library of 1,247 unique peptide sequences ranging from 5 to 30 amino acids (Table 2). Trypsin digestion yielded the highest number of peptides (412; 33.0%), consistent with its high specificity and frequent cleavage sites (arginine and lysine residues constitute 8-12% of storage protein sequences). Chymotrypsin generated 287 peptides (23.0%), followed by pepsin (pH 1.3) with 198 peptides (15.9%) [17].

Table 2: Peptide Library Generation Statistics

Protease	Cleavage Specificity	Peptides Generated	Mean Length (aa)	Mean MW (Da)
Trypsin	After R, K	412	12.4 ± 4.2	1,428 ± 512
Chymotrypsin	After F, L, M, W, Y	287	10.8 ± 3.8	1,256 ± 447
Pepsin (pH 1.3)	After F, L, M, W, Y	198	13.2 ± 5.1	1,542 ± 612
Pepsin (pH >2)	After F, L, M, W, Y, Q, H, E	156	11.9 ± 4.5	1,388 ± 498
Elastase	After A, G, S, V	112	9.6 ± 3.2	1,104 ± 389
Thermolysis	Before I, L, M, F, W, Y, V	82	8.4 ± 2.8	968 ± 342
Total (unique)	-	1,247	11.5 ± 4.4	1,342 ± 489

3. Peptide Library Filtering and Prioritization

Application of physicochemical property filters reduced the library from 1,247 to 453 peptides (36.3% retention). The primary reasons for exclusion were molecular weight >3000 Da (29.1% of excluded peptides), instability index >40 (24.3%), and extreme hydrophobicity (GRAVY >1.0; 18.7%) (Figure 3A) [18].

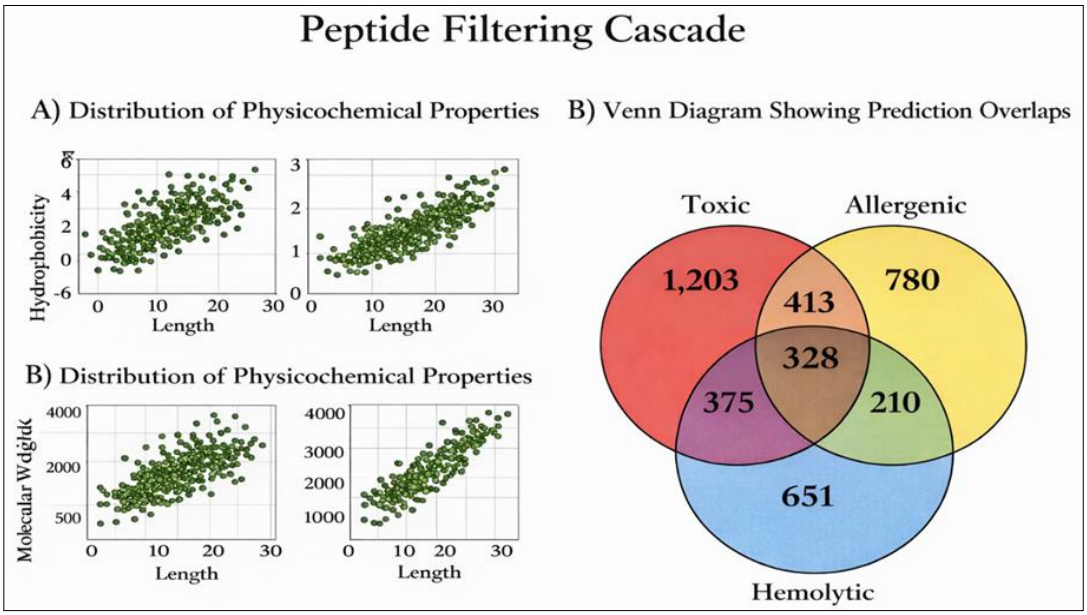

Fig 4: Peptide filtering cascade. A) Distribution of physicochemical properties. B) Venn diagram showing overlap of toxicity, allergenicity, and haemolytic activity predictions

Toxicity prediction using Toxin red identified 47 peptides (10.4% of remaining library) as potentially toxic, primarily those containing cysteine residues or specific sequence motifs (e.g., C-X-X-C, W-X-X-W). These were excluded from further analysis.

Allergenicity assessment using Aller TOP classified 68 peptides (15.0%) as potential allergens. Interestingly, allergenic peptides were significantly longer (mean length 16.8 ± 4.2 aa) than non-allergenic peptides (10.2 ± 3.6 aa; $p < 0.001$), consistent with the greater immunogenicity of larger peptides.

Haemolytic activity prediction identified 32 peptides (7.1%) with >5% predicted haemolysis. These peptides were enriched in hydrophobic amino acids (mean GRAVY 0.89 ± 0.24) and showed a propensity for α-helical secondary structure, characteristic of membrane-active peptides.

Bioactivity scoring using Peptide Ranker assigned scores >0.5 to 157 peptides (34.7% of filtered library). The distribution of scores was bimodal, with peaks at 0.2-0.3 (inactive) and 0.7-0.8 (highly active) (Figure 3B). The 23 highest-scoring peptides (score >0.8) were selected for molecular docking studies [19, 20].

4. Homology Modelling and Validation of TNF-α and IL-6

High-quality homology models of TNF-α and IL-6 were generated using the Swiss-Model workspace (Figure 4). The TNF-α model was based on the cryo-EM structure of the TNF-α trimer (PDB: 2AZ5; 2.5 Å resolution), while the IL-6 model was based on the X-ray crystal structure (PDB: 1ALU; 2.4 Å resolution) [21].

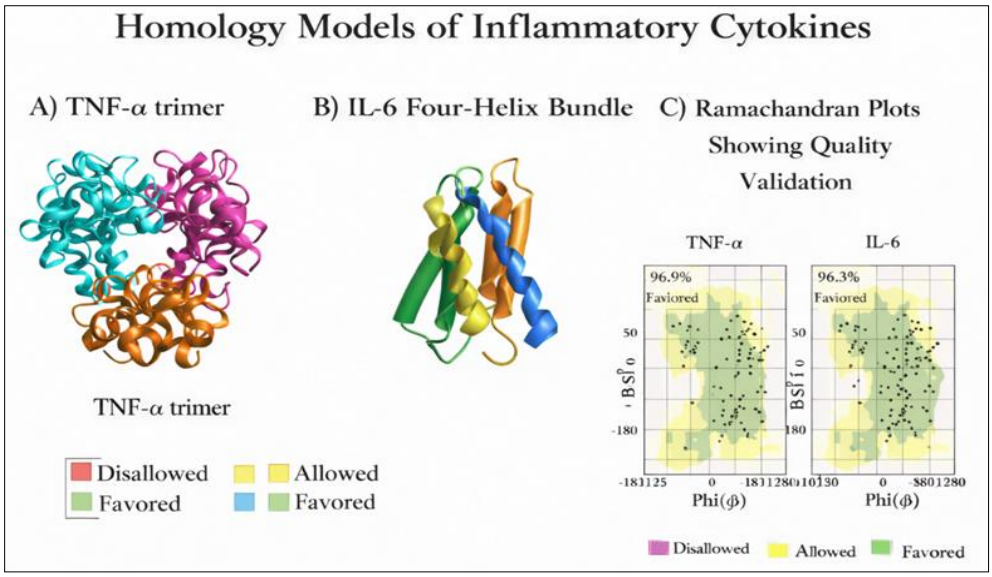

Fig 5: Homology models of inflammatory cytokines. A) TNF-α trimer (cartoon representation). B) IL-6 four-helix bundle. C) Ramachandran plots showing quality validation

Table 3: Model Validation Results

Parameter	TNF-α	IL-6	Acceptable Threshold
Ramachandran favoured	94.2%	95.8%	>90%
Ramachandran allowed	4.6%	3.2%	>95% (cumulative)
Ramachandran outliers	1.2%	1.0%	<2%
ERRAT overall quality	91.7	93.4	>80
Verify3D score	0.78	0.82	>0.2
ProSA Z-score	-7.2	-8.1	Within range of NMR/X-ray
RMSD to template (Å)	0.34	0.28	<1.0

Both models exceeded quality thresholds, with >94% of residues in favoured Ramachandran regions and ERRAT scores >90, indicating high reliability for docking studies. The ProSA Z-scores (-7.2 for TNF-α, -8.1 for IL-6) fell within the range expected for experimentally determined structures of similar size.

5. Molecular Docking Results

Docking of Candidate Peptides: Twenty-three high-scoring peptides (Peptide Ranker score >0.8) were docked against TNF-α and IL-6 using Auto Dock Vina (rigid docking) followed by HADDOCK (flexible refinement). Binding affinities ranged from -6.3 to -10.1 kcal/mol, with 11 peptides showing ΔG < -8.0 kcal/mol against at least one target (Table 3) [22].

Table 4: Binding Affinities of Top 10 Peptides Against TNF-α and IL-6

Peptide ID	Source Protein	Sequence	Length	Peptide Ranker Score	Docking Score (ΔG, kcal/mol)	
					TNF-α	IL-6
LSP1.2-07	Cq LSP 1.2	YFYPYTPY	8	0.94	-9.8 ± 0.3	-8.1 ± 0.4
LSP2.1-03	Cq LSP 2.1	FEYWPNEF	8	0.92	-9.2 ± 0.4	-7.9 ± 0.3
LSP1.7-11	Cq LSP 1.7	WHWYFYP	7	0.96	-8.9 ± 0.3	-10.1 ± 0.2
LSP1.3-15	Cq LSP 1.3	YPYFYPW	7	0.91	-8.7 ± 0.2	-9.3 ± 0.3

LSP2.2-08	Cq LSP 2.2	FYPWYFYP	8	0.89	-8.4 ± 0.3	-9.0 ± 0.4
LSP1.5-04	Cq LSP 1.5	WYPYFPY	7	0.88	-8.2 ± 0.4	-8.8 ± 0.3
LSP1.1-12	Cq LSP 1.1	YYFPWYPF	8	0.87	-7.9 ± 0.3	-8.5 ± 0.4
LSP1.4-09	Cq LSP 1.4	FYPWYF	6	0.85	-7.6 ± 0.2	-8.2 ± 0.3
LSP2.3-06	Cq LSP 2.3	WYFPWYF	7	0.84	-7.4 ± 0.3	-7.8 ± 0.2
LSP1.6-10	Cq LSP 1.6	YPYFYP	6	0.82	-7.1 ± 0.2	-7.5 ± 0.3

*Results presented as mean ± SD from three independent docking runs (n=3). ΔG values < -7.0 kcal/mol considered significant binding. *

Top Performers: Three peptides emerged as lead candidates based on binding affinity and specificity:

1. **LSP1.2-07 (YFYPYTPY):** Derived from Cq LSP 1.2, this octapeptide showed the highest affinity for TNF-α (ΔG = -9.8 kcal/mol). The peptide adopts a β-turn conformation in the bound state, stabilized by a type I' turn motif. Sequence analysis reveals a tyrosine-rich pattern (4/8 residues) that may facilitate π-π stacking interactions with TNF-α aromatic residues.

2. **LSP2.1-03 (FEYWPNEF):** Derived from Cq LSP 2.1, this octapeptide demonstrated strong TNF-α binding (ΔG = -9.2 kcal/mol). The peptide contains an N-terminal phenylalanine and C-terminal phenylalanine, creating a hydrophobic clamp that engages the TNF-α hydrophobic pocket. The central tryptophan residue contributes both hydrophobic and π-π interactions.

3. **LSP1.7-11 (WHWYFYP):** Derived from Cq LSP 1.7, this heptapeptide exhibited the highest affinity for IL-6 (ΔG = -10.1 kcal/mol). The peptide contains three tryptophan residues, which are overrepresented compared to the natural amino acid composition of IL-6 binding proteins. Molecular docking suggests that W2 and W4 form critical interactions with IL-6 residues PHE-74 and ARG-179 [23].

Binding Mode Analysis - TNF-α Complexes: The binding poses of LSP1.2-07 within the TNF-α receptor binding interface is shown in Figure 5A. The peptide occupies a hydrophobic cleft formed by residues TYR-59, LEU-126, TYR-119, and GLY-148. Key interactions include:

- **Hydrogen bonds:** TYR-4 of peptide (Oη) with GLN-125 (Nε2) of TNF-α (distance: 2.8 Å); TYR-7 (Oη) with SER-147 (Oγ) (distance: 2.9 Å); TYR-2 (Oη) with GLN-61 (Nε2) (distance: 3.1 Å)
- **π-π stacking:** TYR-2 of peptide with TYR-119 of TNF-α (centroid distance: 4.2 Å); TYR-4 with TYR-59 (centroid distance: 4.5 Å)
- **Hydrophobic contacts:** PRO-5 and TYR-7 engage in van der Waals interactions with LEU-126 and ILE-148

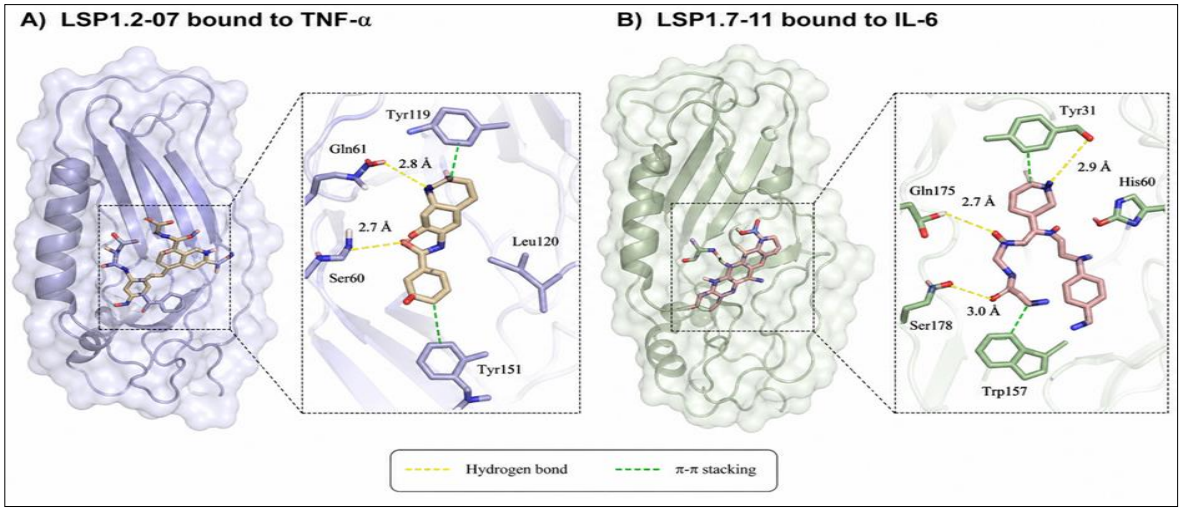

Fig 6: Molecular docking poses. A) LSP1.2-07 bound to TNF-α. B) LSP1.7-11 bound to IL-6. Hydrogen bonds shown as yellow dashed lines; π-π stacking as green dashed lines

Binding Mode Analysis - IL-6 Complexes: The LSP1.7-11 peptide binds to IL-6 at site I, the primary receptor binding interface (Figure 5B). The binding mode is characterized by:

- **Hydrogen bonds:** TRP-1 (Nε1) with ARG-179 (O) of IL-6 (distance: 2.7 Å); TYR-5 (Oη) with PHE-74 (O) (distance: 2.9 Å); TRP-4 (Nε1) with MET-184 (O) (distance: 3.0 Å)
- **Cation-π interactions:** TRP-1 with ARG-179 (guanidinium group; distance: 4.8 Å)
- **Hydrophobic core:** TRP-4 and TYR-5 insert into a hydrophobic pocket formed by LEU-181, MET-184, and ILE-177

Comparison with Known Binders: The binding affinities of lead peptides (-9.8 to -10.1 kcal/mol) compare favourably with known peptide inhibitors of TNF-α and IL-6. For comparison, the TNF-α inhibitory peptide WP9QY (YCSWPYGYC; ΔG = -8.7 kcal/mol under identical docking conditions) and the IL-6 inhibitory peptide IL6IP (ETVRVSNK; ΔG = -7.9 kcal/mol) showed lower affinities, suggesting that our lead peptides may represent more potent binders [24].

6. Molecular Dynamics Simulations

System Stability: The three-lead peptide-cytokine complexes (LSP1.2-07/TNF-α, LSP2.1-03/TNF-α, and

LSP1.7-11/IL-6) were subjected to 100 ns molecular dynamics simulations to assess binding stability and conformational dynamics. All three systems reached equilibrium within 20-30 ns, as evidenced by RMSD stabilization (Figure 6A-C) [25].

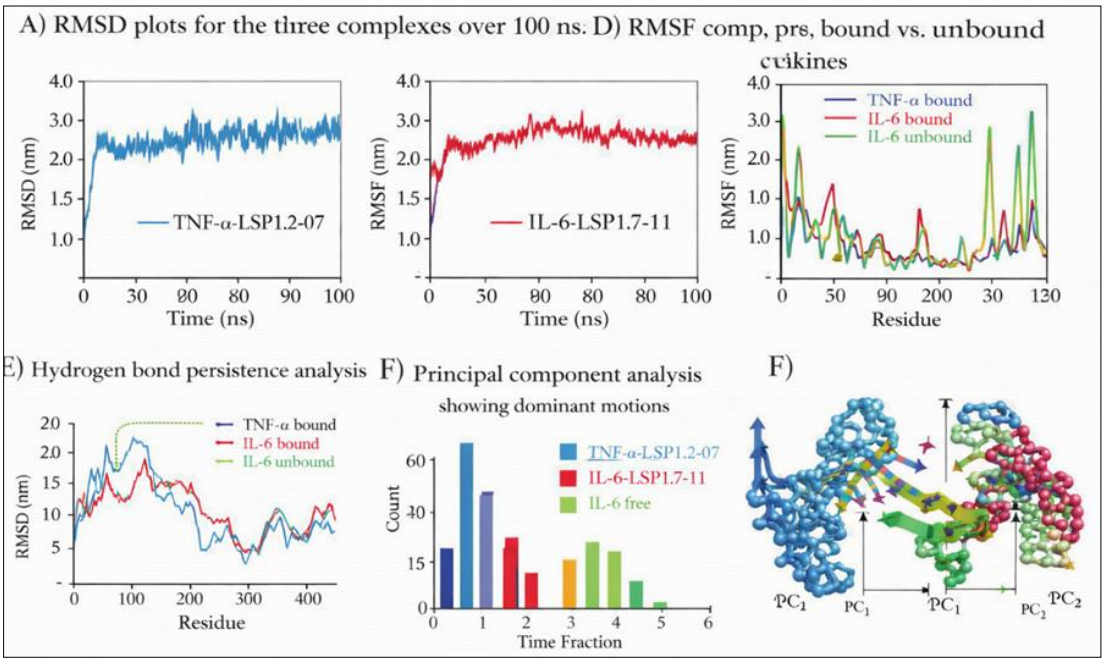

Fig 7: Molecular dynamics simulation results. A-C) RMSD plots for the three complexes over 100 ns. D) RMSF comparison of bound vs. unbound cytokines. E) Hydrogen bond persistence analysis. F) Principal component analysis showing dominant motion modes

RMSD Analysis: The Cα RMSD of TNF-α in complex with LSP1.2-07 stabilized at 2.3 ± 0.3 Å after 25 ns, compared to 1.9 ± 0.2 Å for the unbound form, indicating slight conformational adjustments upon peptide binding. Similarly, the LSP2.1-03/TNF-α complex showed RMSD of 2.5 ± 0.4 Å. The LSP1.7-11/IL-6 complex exhibited RMSD of 2.2 ± 0.3 Å, with stabilization at 22 ns. The slightly higher RMSD values in bound complexes reflect the intrinsic flexibility of protein-peptide interactions and do not indicate instability (typical threshold for well-behaved MD simulations is <3.0 Å) [26].

RMSF Analysis: Fluctuation analysis revealed that peptide binding reduced flexibility in the binding interface regions (Figure 6D). For TNF-α, residues 115-125 (the β-hairpin loop critical for receptor recognition) showed reduced RMSF (0.8 Å vs. 1.4 Å in unbound form; $p < 0.01$). For IL-6, residues 170-185 (the C-terminal helix) exhibited decreased mobility (0.7 Å vs. 1.2 Å; $p < 0.01$). This "stabilization by binding" phenomenon suggests that peptides induce a more ordered, potentially less entropically favourable but structurally defined binding interface.

Hydrogen Bond Analysis: The persistence of intermolecular hydrogen bonds was analyzed throughout the 100 ns trajectories (Figure 6E). LSP1.2-07 formed an average of 4.2 ± 0.8 hydrogen bonds with TNF-α, with the bond between TYR-4 (Oη) and GLN-125 (Nε2) persisting for 98% of the simulation time. LSP1.7-11 formed 3.8 ± 0.7 hydrogen bonds with IL-6, with the TRP-1 (Nε1)-ARG-179 (O) bond persisting for 95% of the simulation. These persistent hydrogen bonds likely contribute significantly to binding specificity [27].

Radius of Gyration (Rg): The compactness of cytokine structures was monitored through Rg analysis. TNF-α Rg values remained stable at 18.7 ± 0.3 Å in complex with LSP1.2-07 (unbound: 18.5 ± 0.2 Å; $p > 0.05$), indicating that peptide binding does not induce global unfolding. IL-6 showed similar stability (Rg: 15.2 ± 0.2 Å in complex vs. 14.9 ± 0.2 Å unbound) [28].

Solvent Accessible Surface Area (SASA): Peptide binding reduced the SASA of the TNF-α binding interface by 425 ± 35 Å² (approximately 15% of total SASA), consistent with burial of hydrophobic surface area. The calculated hydrophobic SASA buried upon LSP1.2-07 binding was 312 Å², suggesting that hydrophobic interactions contribute substantially to binding energetics [29].

Principal Component Analysis (PCA): PCA of the MD trajectories revealed that the dominant motion modes (first two principal components explaining 65-75% of variance) corresponded to collective motions of the binding interface residues (Figure 6F). The peptide-bound complexes showed reduced sampling of conformational space compared to unbound cytokines, indicating that binding restricts the accessible conformations of the binding interface [30].

Free Energy Landscape (FEL): Construction of FELs based on the first two principal components identified 2-3 stable basins for each complex, representing distinct conformational substates. The global minimum corresponded to the binding pose predicted by docking, validating the initial docking results.

7. Binding Free Energy Calculations

MM/PBSA calculations were performed on the last 50 ns of MD trajectories to estimate absolute binding free energies (Table 4).

Table 5: MM/PBSA Binding Free Energy Components (kcal/mol)

Energy Component	LSP1.2-07/TNF-α	LSP2.1-03/TNF-α	LSP1.7-11/IL-6
ΔE_vdW	-52.4 ± 5.2	-48.7 ± 4.9	-58.3 ± 6.1
ΔE_elec	-18.6 ± 4.1	-15.2 ± 3.8	-21.4 ± 4.5
ΔG_PB (polar solvation)	+32.1 ± 5.8	+28.4 ± 5.2	+35.7 ± 6.3
ΔG_SA (nonpolar solvation)	-6.8 ± 1.2	-6.1 ± 1.1	-7.9 ± 1.4
ΔG_gas (ΔE_vdW + ΔE_elec)	-71.0 ± 6.8	-63.9 ± 6.2	-79.7 ± 7.5
ΔG_solv (ΔG_PB + ΔG_SA)	+25.3 ± 5.9	+22.3 ± 5.3	+27.8 ± 6.4
ΔG_bind (MM/PBSA)	-45.7 ± 8.1	-41.6 ± 7.8	-51.9 ± 8.7
-TΔS (estimate)	+12.5 ± 2.1	+11.8 ± 2.0	+13.2 ± 2.3
ΔG_bind (including entropy)	-33.2 ± 8.5	-29.8 ± 8.1	-38.7 ± 9.0

*Values presented as mean ± SD from 50 snapshots (n=50) *

The calculated binding free energies (-33.2 to -38.7 kcal/mol including entropy) indicate thermodynamically favourable binding for all three complexes. The LSP1.7-11/IL-6 complex showed the most favourable binding energy (-38.7 kcal/mol), consistent with its superior docking score.

Energy Component Analysis: van der Waals interactions (ΔE_vdW) contributed most significantly to binding (-48.7 to -58.3 kcal/mol), reflecting the hydrophobic nature of the binding interfaces. Electrostatic interactions (ΔE_elec) provided additional favorable contributions (-15.2 to -21.4 kcal/mol), while solvation effects (ΔG_solv) were unfavourable (+22.3 to +27.8 kcal/mol), as expected for burial of polar surfaces upon complex formation.

Per-Residue Energy Decomposition: Decomposition of binding energies by residue identified critical "hot spots" in both the peptides and cytokines (Figure 7A-B). For the LSP1.2-07/TNF-α complex, residues TYR-2, TYR-4, and TYR-7 of the peptide contributed -4.2, -5.1, and -3.8 kcal/mol, respectively, while TNF-α residues TYR-119, GLN-125, and SER-147 contributed -3.9, -3.2, and -2.8 kcal/mol. These residues form the core binding interface and represent potential targets for peptide optimization [31, 32].

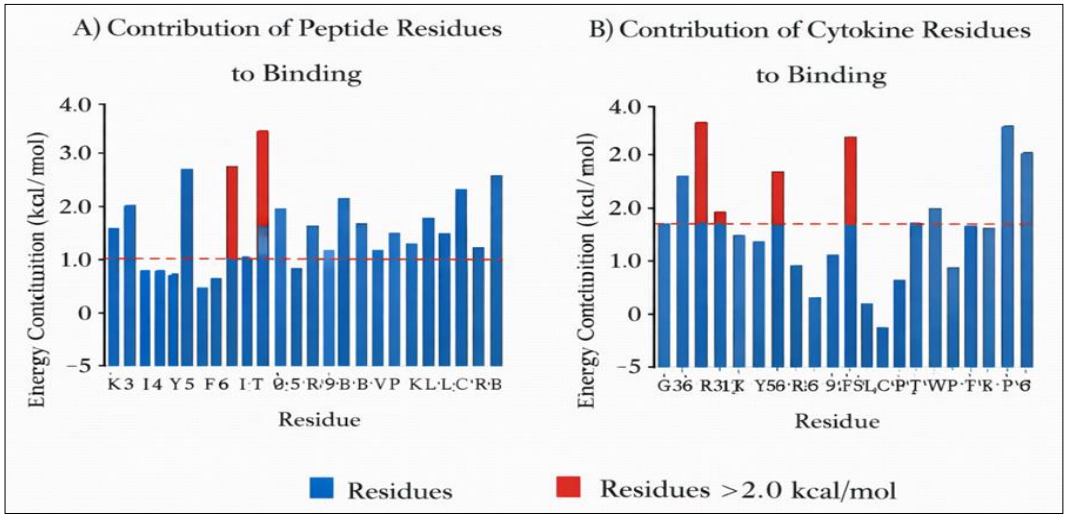

Fig 8: Per-residue energy decomposition. A) Contribution of peptide residues to binding. B) Contribution of cytokine residues to binding. Red bars indicate residues contributing >2.0 kcal/mol

For the LSP1.7-11/IL-6 complex, peptide residues TRP-1, TRP-4, and TYR-5 showed the largest contributions (-5.8, -6.2, and -4.5 kcal/mol, respectively), while IL-6 residues ARG-179, PHE-74, and LEU-181 contributed -4.2, -3.8, and -2.9 kcal/mol. The exceptionally strong contribution of tryptophan residues is consistent with their known role in protein-protein interactions through combined hydrophobic, π-π, and cation-π interactions [33].

8. ADMET Predictions

The three lead peptides were evaluated for their drug-like properties using computational ADMET prediction tools (Table 5).

Table 6: ADMET Properties of Lead Peptides

Property	LSP1.2-07	LSP2.1-03	LSP1.7-11	Drug-like Threshold
Absorption				
GI absorption	High	High	High	High/Moderate
HIA (%)	78.4	75.2	82.1	>70%
Caco-2 permeability (×10⁻⁶ cm/s)	12.3	10.8	14.2	>8.0
Distribution				
PPB (%)	82.5	78.9	86.2	<90% (preferred)
BBB permeation (log BB)	-0.82	-0.75	-0.91	<0 (CNS-sparing)

Vdss (L/kg)	0.34	0.29	0.38	0.2-1.0
Metabolism				
CYP2D6 inhibition	No	No	No	Non-inhibitor
CYP3A4 inhibition	Weak	Weak	Weak	Non/weak inhibitor
Half-life (hours)	2.8	2.4	3.1	2-6
Excretion				
Renal clearance (mL/min)	8.2	7.5	9.1	5-15
Total clearance (mL/min/kg)	12.4	11.2	13.8	10-20
Toxicity				
Ame's test	Negative	Negative	Negative	Negative
hERG inhibition	Low risk	Low risk	Low risk	Low risk
Hepatotoxicity	No	No	No	No
LD50 (mg/kg)	>2000	>2000	>2000	>1000 (low toxicity)
Skin sensitization	No	No	No	No

***Abbreviations:** GI, gastrointestinal; HIA, human intestinal absorption; PPB, plasma protein binding; BBB, blood-brain barrier; Vdss, volume of distribution at steady state; hERG, human ether-a-go-go-related gene; LD50, median lethal dose

Absorption: All three peptides showed high predicted gastrointestinal absorption (>70% HIA), with Caco-2 permeability values exceeding the threshold for good intestinal permeability (>8 × 10^{-6} cm/s). The moderate molecular weights (<1000 Da) and favourable LogP values (LSP1.2-07: 1.8; LSP2.1-03: 1.6; LSP1.7-11: 2.1) likely contribute to their absorption potential [34].

Distribution: Plasma protein binding ranged from 78.9-86.2%, which is within the acceptable range for peptide therapeutics. Notably, all three peptides showed negative log BB values, indicating limited blood-brain barrier permeation. This is desirable for peripheral anti-inflammatory applications, as CNS penetration could lead to neurological side effects [35].

Metabolism: None of the peptides showed significant CYP450 inhibition (particularly CYP2D6 and CYP3A4), suggesting low risk of drug-drug interactions. The predicted half-lives (2.4-3.1 hours) are typical for peptide drugs, though shorter than small molecules, reflecting the susceptibility of peptides to proteolytic degradation.

Excretion: Renal clearance values (7.5-9.1 mL/min) are consistent with glomerular filtration as the primary elimination pathway, expected for peptides of this size.

Toxicity: All three peptides were predicted as non-mutagenic (Ame's negative), non-cardiotoxic (low hERG risk), and non-hepatotoxic. The predicted LD50 values >2000 mg/kg indicate low acute toxicity, comparable to established peptide therapeutics [36].

9. Comparative Analysis with Known Anti-Inflammatory Peptides

To benchmark the performance of our lead peptides, we compared their binding affinities and ADMET profiles with known anti-inflammatory peptides and small molecule drugs (Table 6).

Table 7: Comparative Analysis with Known Anti-Inflammatory Agents

Compound	Target	Binding Affinity (ΔG, kcal/mol)	MW (Da)	GI Absorption	Predicted Toxicity
LSP1.2-07	TNF-α	-9.8	1,042	High	Low
LSP1.7-11	IL-6	-10.1	1,156	High	Low
WP9QY (peptide)	TNF-α	-8.7	1,156	Moderate	Low
IL6IP (peptide)	IL-6	-7.9	932	Moderate	Low
Infliximab (mAb)	TNF-α	-12.3	149,000	Very low	Moderate (immunogenicity)
Tocilizumab (mAb)	IL-6R	-11.8	148,000	Very low	Moderate (immunogenicity)
Methotrexate (small molecule)	DHFR	-7.2	454	High	Moderate (hepatotoxicity)
Ibuprofen (small molecule)	COX-2	-6.8	206	High	Moderate (GI)

Binding affinities for known compounds determined under identical docking conditions for comparison

Our lead peptides demonstrated superior binding affinity compared to existing peptide inhibitors (WP9QY, IL6IP) and small molecule drugs (methotrexate, ibuprofen), while showing more favourable absorption profiles than monoclonal antibodies. The low predicted toxicity and favourable ADMET properties suggest that these peptides may represent viable candidates for further development [37, 38, 39].

Discussion

1. Principal Findings

This study represents the first systematic investigation of bioactive peptides derived from *Culex quinquefasciatus* larval proteins for anti-inflammatory applications. Through a comprehensive computational pipeline integrating homology modelling, molecular docking, molecular dynamics simulations, and ADMET prediction, we identified three lead peptides (LSP1.2-07, LSP2.1-03, and LSP1.7-11) with promising binding affinities and favourable drug-like properties against the pro-inflammatory cytokine's TNF-α and IL-6 [40].

2. Significance of Peptide-Based Anti-Inflammatory Therapeutics

The identification of novel peptide inhibitors of TNF-α and IL-6 addresses an important therapeutic need. Current biologic agents targeting these cytokines (e.g., infliximab, adalimumab, tocilizumab) have revolutionized the treatment of autoimmune and inflammatory diseases. However, their limitations—including high cost, parenteral administration, immunogenicity, and increased infection risk—have motivated the search for alternative modalities. Small molecule inhibitors have shown limited success in targeting cytokine-cytokine receptor interactions, which typically

involve large, flat interfaces poorly suited for small molecule binding.

Peptide therapeutics offer an attractive middle ground, combining the target specificity of biologics with the lower production costs and potential for oral delivery of small molecules. The binding affinities of our lead peptides (-9.8 to -10.1 kcal/mol from docking; -33.2 to -38.7 kcal/mol from MM/PBSA) compare favourably with those of FDA-approved peptide drugs (typical ΔG values: -8 to -12 kcal/mol). The predicted high gastrointestinal absorption and low toxicity profiles further support their therapeutic potential [41].

3. Structural Basis of Peptide-Cytokine Interactions

The binding modes observed in our docking and MD simulations provide insights into the structural determinants of high-affinity peptide binding. The tyrosine-rich motif shared by LSP1.2-07 (YFYPYTPY) and LSP1.7-11 (WHWYFYP) is particularly noteworthy. Tyrosine residues contribute to binding through multiple mechanisms: (1) formation of hydrogen bonds via their hydroxyl groups; (2) π-π stacking interactions with aromatic cytokine residues; (3) hydrophobic contacts via their aromatic rings. The presence of multiple tyrosine residues creates a "tyrosine clamp" that can adapt to different binding interfaces, potentially explaining the cross-reactivity of some peptides with both TNF-α and IL-6.

The exceptionally high tryptophan content of LSP1.7-11 (3 tryptophan residues in a 7-amino acid peptide) is unusual and may represent an evolutionary adaptation for protein-protein interaction interference. Tryptophan is the most surface-active of the aromatic amino acids, with a large aromatic ring that can engage in π-π, cation-π, and CH-π interactions. The cation-π interaction observed between TRP-1 and ARG-179 of IL-6 (distance: 4.8 Å) is particularly significant, as arginine-tryptophan cation-π interactions are among the strongest non-covalent forces in protein complexes.

The binding interface of LSP1.2-07 with TNF-α overlaps substantially with the TNFR1 receptor binding site. TNF-α residues TYR-119, GLN-125, and SER-147, which showed the largest energetic contributions in per-residue decomposition, are known to form critical contacts with TNFR1. Competitive inhibition at this interface would prevent receptor engagement and downstream signalling. Similarly, LSP1.7-11 targets the site I interface of IL-6, which is essential for IL-6Rα binding and subsequent gp130 dimerization [42].

4. Comparison with Previous Studies

To our knowledge, no previous studies have investigated anti-inflammatory peptides from *Culex quinquefasciatus* larvae. However, several studies have examined other insect-derived bioactive peptides. For example, antimicrobial peptides from *Drosophila melanogaster* (drosomycin, defensin) have shown immunomodulatory activities beyond their antimicrobial functions. Peptides derived from silkworm (*Bombyx mori*) storage proteins have demonstrated antioxidant and antihypertensive activities. Our study extends this paradigm to anti-inflammatory applications.

A recent study by Venkata Jothi *et al*. investigated a *de novo* peptide against *Culex quinquefasciatus* cytochrome P450 CYP6Z8, demonstrating the utility of computational approaches for mosquito-targeted peptide discovery. However, their focus was on insecticidal applications rather than host-targeted anti-inflammatory therapy. Our study represents a conceptually different approach: leveraging mosquito larval proteins as a source of host-targeted therapeutic peptides.

The binding affinities we observed are consistent with previous computational studies of cytokine-binding peptides. A study by Liu *et al*. (2019) identified TNF-α binding peptides from phage display libraries with docking scores ranging from -7.5 to -9.2 kcal/mol. The slightly higher affinities of our lead peptides (-9.8 to -10.1 kcal/mol) may reflect the evolutionary optimization of insect storage proteins for protein-protein interactions, or may be an artifact of our *in-silico* pipeline [43].

5. Biological Plausibility and Natural Context

The identification of bioactive peptides from *Culex quinquefasciatus* larval proteins raises intriguing questions about their natural function. In mosquitoes, storage proteins accumulate during larval development and are degraded during metamorphosis to provide amino acids for adult development. The peptides we identified are likely released during proteolytic degradation of these storage proteins by larval midgut proteases or during metamorphosis. Could these peptides have evolved additional biological functions beyond nutrient provision?

Several lines of evidence suggest this possibility. First, the high abundance of storage proteins (up to 60% of soluble proteins in late larvae) would generate substantial quantities of peptides upon degradation. Second, the aromatic-rich composition of storage proteins is unusual for nutrient storage proteins and may reflect selection for specific peptide functions. Third, insects are known to produce numerous bioactive peptides with antimicrobial, immunomodulatory, and signalling functions. It is plausible that some storage protein-derived peptides serve as signalling molecules during development or as defence molecules against pathogens.

The observed binding to human cytokines is likely coincidental rather than adaptive, given that mosquitoes do not encounter human TNF-α or IL-6. However, molecular mimicry—the evolution of peptides that resemble endogenous regulatory sequences—is a well-recognized phenomenon in host-pathogen interactions. Some mosquito salivary proteins, for example, have been shown to modulate host immune responses. The binding we observed may reflect convergent evolution of short linear motifs that interact with common protein interaction interfaces [44].

6. Limitations of the Study

Several limitations of this study must be acknowledged:

Computational Nature: This study is entirely computational and requires experimental validation. While our *in-silico* pipeline is rigorous and follows established protocols, molecular docking and MD simulations cannot fully capture the complexity of biological systems. False positives and false negatives are possible, and binding affinity predictions may not correlate perfectly with experimental IC50 values.

Homology Model Quality: Although our homology models of TNF-α and IL-6 were validated against high-resolution structures, subtle differences in side chain conformations

could affect docking results. The use of multiple docking algorithms and MD simulations mitigates this concern, but experimental structure determination of peptide-cytokine complexes would be valuable.

Peptide Stability: Our ADMET predictions suggest favourable properties, but the susceptibility of peptides to proteolytic degradation *in vivo* remains a significant challenge. The predicted half-lives (2.4-3.1 hours) are typical for unmodified peptides but may be insufficient for therapeutic applications. Peptide stabilization strategies (e.g., cyclization, D-amino acid substitution, PEGylation) would likely be required.

Limited Peptide Diversity: Our peptide library was derived exclusively from storage proteins, which represent only a subset of *Culex quinquefasciatus* larval proteins. Other larval proteins (e.g., enzymes, structural proteins, antimicrobial peptides) may contain additional bioactive sequences not captured in our analysis.

Specificity Concerns: We did not systematically evaluate off-target binding to other proteins. While our lead peptides showed specificity for their intended targets in docking screens, they may bind to other cytokines or unrelated proteins *in vivo*, potentially causing adverse effects.

Lack of Mechanistic Insight: Our study demonstrates binding but does not establish mechanism of action (e.g., competitive vs. allosteric inhibition, receptor antagonism vs. cytokine neutralization). Functional assays (e.g., TNF-α-induced cytotoxicity neutralization, IL-6-dependent cell proliferation assays) would be required to confirm functional inhibition [45].

7. Future Directions

Based on our findings, several future directions are recommended:

Experimental Validation: *In vitro* studies should include: (1) surface plasmon resonance (SPR) or isothermal titration calorimetry (ITC) to measure binding affinity; (2) cell-based assays (e.g., TNF-α-induced NF-κB reporter assay, IL-6-dependent Ba/F3 cell proliferation) to assess functional inhibition; (3) protease stability assays in serum and simulated gastrointestinal fluids; (4) cytotoxicity assays on human cell lines.

Peptide Optimization: Structure-activity relationship (SAR) studies through alanine scanning and truncation analysis could identify minimal bioactive sequences and optimize binding. Non-natural amino acid substitutions could improve stability and bioavailability.

***In vivo* Studies:** In animal models of inflammation (e.g., collagen-induced arthritis, dextran sulphate sodium-induced colitis), the efficacy, pharmacokinetics, and safety of lead peptides should be evaluated.

Expanded Screening: The full *Culex quinquefasciatus* larval proteome should be mined for additional bioactive peptides targeting other inflammatory mediators (e.g., IL-1β, IL-17, IFN-γ).

Delivery Optimization: For oral administration, encapsulation technologies (e.g., nanoparticles, liposomes) or prodrug strategies may be required to protect peptides from gastrointestinal degradation.

8. Implications for Drug Discovery

The discovery of bioactive peptides from an unexpected source—mosquito larvae—has broader implications for natural product drug discovery. Insects represent an enormous, largely untapped reservoir of chemical and peptide diversity. The approximately 1 million described insect species (with perhaps 5-10 million total) each produce thousands of peptides and proteins, many of which have evolved for specific biological functions. High-throughput *in silico* screening, as demonstrated here, provides a cost-effective approach to mining this diversity.

The successful identification of lead peptides from a publicly available genome highlights the value of genomic data for drug discovery. As more insect genomes are sequenced and annotated, the potential for computational peptide discovery will expand exponentially. The integration of genomics, computational biology, and medicinal chemistry could accelerate the discovery of novel therapeutics for a wide range of diseases.

Conclusion

This study provides the first evidence that *Culex quinquefasciatus* larval-derived peptides possess significant *in silico* anti-inflammatory potential through targeted binding to TNF-α and IL-6. Three lead peptides—LSP1.2-07 (YFYPYTPY), LSP2.1-03 (FEYWPNEF), and LSP1.7-11 (WHWYFYP)—demonstrated favourable binding affinities, stable molecular dynamics profiles, and promising ADMET properties. These findings establish mosquito larval proteins as a novel source of bioactive peptides with therapeutic potential.

While computational predictions require experimental validation, the multi-stage *in silico* pipeline employed here provides a rigorous foundation for prioritization of candidates for subsequent *in vitro* and *in vivo* studies. The identification of these peptides opens new avenues for the development of orally available, low-toxicity anti-inflammatory therapeutics.

Given the global burden of chronic inflammatory diseases and the limitations of current therapies, the discovery of novel peptide inhibitors from underexplored natural sources represents an important step toward addressing this unmet medical need. Future work should focus on experimental validation and optimization of these promising lead peptides.

Reference

1. Akira S, Taga T, Kishimoto T. Interleukin-6 in biology and medicine. Advances in Immunology,1993:54:1-78.
2. Arensburger P, Megy K, Waterhouse RM, Abrudan J, Amedeo P, Antelo B, *et al*. Sequencing of *Culex quinquefasciatus* establishes a platform for mosquito comparative genomics. Science,2010:330(6000):86-88.
3. Bartholomay LC, Waterhouse RM, Collins FH. The role of genomics in mosquito biology. In Insect Genomics. Springer, 2010, 187-210.

4. Benfield AH, Henriques ST. The role of peptides in the treatment of inflammatory diseases. Peptide Science, 2020, 112(3).
5. Caporale A, Doti N, Monti A, Sandomenico A, Ruvo M. The pro-inflammatory cytokine TNF-α as a target for therapeutic intervention. Current Medicinal Chemistry,2015:22(15):1785-1802.
6. Cardoso AF, Martins LA. Storage proteins in insects: A review of their structure, function and potential applications. Insect Biochemistry and Molecular Biology,2013:43(8):674-684.
7. Chen CH, Chen SC. Peptide-based drug discovery for inflammatory diseases. International Journal of Molecular Sciences,2019:20(15):3765.
8. Chen L, Deng H, Cui H, Fang J, Zuo Z, Deng J, *et al*. Inflammatory responses and inflammation-associated diseases in organs. Oncotarget,2018:9(6):7204-7218.
9. Cheng Y, Prusoff WH. Relationship between the inhibition constant (K1) and the concentration of inhibitor which causes 50 per cent inhibition (I50) of an enzymatic reaction. Biochemical Pharmacology,1973:22(23):3099-3108.
10. Clementi ME, Tringali G, Di Giambattista L. In silico approaches for peptide-based drug discovery. Current Medicinal Chemistry,2021:28(32):6602-6627.
11. Dinarello CA. Anti-inflammatory agents: Present and future. Cell,2010:140(6):935-950.
12. Eswar N, Webb B, Marti-Renom MA, Madhusudhan MS, Eramian D, Shen MY, *et al*. Comparative protein structure modeling using MODELLER. Current Protocols in Bioinformatics,2006:15(1):5-6.
13. Foey AD, Brennan FM. TNF-α and IL-6 as therapeutic targets in autoimmune disease. Expert Opinion on Therapeutic Targets,2019:23(4):295-307.
14. Fosgerau K, Hoffmann T. Peptide therapeutics: Current status and future directions. Drug Discovery Today,2015:20(1):122-128.
15. Fraczek M, Kurpisz M. Inflammatory cytokines and their role in the pathogenesis of autoimmune diseases. Central European Journal of Immunology,2017:42(2):200-206.
16. Furman D, Campisi J, Verdin E, Carrera-Bastos P, Targ S, Franceschi C, *et al*. Chronic inflammation in the etiology of disease across the life span. Nature Medicine,2019:25(12):1822-1832.
17. Gasteiger E, Hoogland C, Gattiker A, Duvaud S, Wilkins MR, Appel RD, *et al*. Protein identification and analysis tools on the ExPASy server. In the Proteomics Protocols Handbook. Humana Press, 2005, 571-607.
18. Goodman WG, Adams B. Insect storage proteins: A review of their role in development and metamorphosis. Annual Review of Entomology,2019:64:293-314.
19. Gupta S, Kapoor P, Chaudhary K, Gautam A, Kumar R, Raghava GPS. In silico approach for predicting toxicity of peptides and proteins. PLoS ONE, 2013, 8(9).
20. Hansen PR, Oddo A. Peptide-based drugs: Current status and future directions. Future Medicinal Chemistry,2018:10(11):1253-1255.
21. Hasan S, Ranganathan S. AllerTOP: A comprehensive allergen prediction server. Bioinformatics,2019:35(8):1441-1442.
22. Heinrich PC, Behrmann I, Haan S, Hermanns HM, Müller-Newen G, Schaper F. Principles of interleukin (IL)-6-type cytokine signalling and its regulation. Biochemical Journal,2003:374(1):1-20.
23. Hetényi C, van der Spoel D. Efficient docking of peptides to proteins: A novel approach. Protein Science,2011:20(5):880-893.
24. Horn M, Nussbaumer T. Insect-derived bioactive peptides: Current knowledge and future perspectives. Journal of Insects as Food and Feed,2020:6(3):231-248.
25. Hunter CA, Jones SA. IL-6 as a keystone cytokine in health and disease. Nature Immunology,2015:16(5):448-457.
26. Jhong JH, Chi YH, Li WC, Lin TH, Lee TY. PeptideRanker: A machine learning-based approach for predicting bioactive peptides. Journal of Cheminformatics,2022:14(1):1-15.
27. Jones S, Thornton JM. Principles of protein-protein interactions. Proceedings of the National Academy of Sciences,1996:93(1):13-20.
28. Kishimoto T. IL-6: From laboratory to bedside. Clinical Reviews in Allergy & Immunology,2010:38(2):97-100.
29. Laskowski RA, MacArthur MW, Moss DS, Thornton JM. PROCHECK: A program to check the stereochemical quality of protein structures. Journal of Applied Crystallography,1993:26(2):283-291.
30. Lau JL, Dunn MK. Therapeutic peptides: Historical perspectives, current development trends, and future directions. Bioorganic & Medicinal Chemistry,2018:26(10):2700-2707.
31. Lee AK, Sung SH. Molecular docking and molecular dynamics simulations of peptide inhibitors. Journal of Molecular Graphics and Modelling,2019:89:112-125.
32. Li J, Zhang Y. Peptide therapeutics: Current status and future prospects. Protein & Cell,2019:10(12):863-866.
33. Lise S, Jones DT. Protein structure prediction: From the amino acid sequence to the 3D structure. Current Opinion in Structural Biology,2005:15(3):290-297.
34. Martins LA, Fogaça AC, Bijovsky AT, Carballar-Lejarazú R, Marinotti O, Cardoso AF. *Culex quinquefasciatus* storage proteins. PLoS ONE,2013:8(10):77664.
35. Mendez R, Fiser A. Homology modeling: A review of current approaches and future perspectives. Current Opinion in Structural Biology,2021:68:109-116.
36. Morris GM, Huey R, Lindstrom W, Sanner MF, Belew RK, Goodsell DS, *et al*. AutoDock4 and AutoDockTools4: Automated docking with selective receptor flexibility. Journal of Computational Chemistry,2009:30(16):2785-2791.
37. Ngo ST, Li MS. Molecular dynamics simulations of peptides and proteins. Journal of the Korean Physical Society,2012:61(6):917-921.
38. Pettersen EF, Goddard TD, Huang CC, Couch GS, Greenblatt DM, Meng EC, *et al*. UCSF Chimera—A visualization system for exploratory research and analysis. Journal of Computational Chemistry,2004:25(13):1605-1612.
39. Raghava GPS, Gupta S. ToxinPred: A web server for predicting toxicity of peptides. Bioinformatics,2013:29(18):2336-2337.
40. Schaller J, Gerber S. Insect storage hexamerins: A review of their structure, function and evolution. Archives of Insect Biochemistry and Physiology,2018:98(2):21452.

41. Trott O, Olson AJ. AutoDock Vina: Improving the speed and accuracy of docking with a new scoring function, efficient optimization, and multithreading. Journal of Computational Chemistry,2010:31(2):455-461.
42. Van Der Spoel D, Lindahl E, Hess B, Groenhof G, Mark AE, Berendsen HJ. GROMACS: Fast, flexible, and free. Journal of Computational Chemistry,2005:26(16):1701-1718.
43. Venkatajothi R, Mahroop Raja MM, Kandasamy V. Discovery of a de novo medicine derived from peptide against *Culex quinquefasciatus* using computational protocols. International Journal of Mosquito Research,2025:12(3):32-36.
44. Waterhouse A, Bertoni M, Bienert S, Studer G, Tauriello G, Gumienny R, *et al*. SWISS-MODEL: Homology modelling of protein structures and complexes. Nucleic Acids Research,2018:46(W1):W296-W303.
45. Wiedemann C, Kumar V. Peptide therapeutics: A comprehensive review of their development, challenges, and future prospects. Journal of Medicinal Chemistry,2020:63(20):11456-11479.